Geoscience Frontiers 8 (2017) 189–197

Contents lists available at ScienceDirect

China University of Geosciences (Beijing)

Geoscience Frontiers

journal homepage: www.elsevier.com/locate/gsf

Research paper

Application of fractal content-gradient method for delineating geochemical anomalies associated with copper occurrences in the Yangla ore field, China

Zhen Chen, Jianping Chen*, Shufang Tian, Bin Xu

School of Earth Sciences and Resources, China University of Geosciences, 29 Xueyuan Road, Beijing 100083, China

ARTICLE INFO

Article history:
Received 8 August 2015
Received in revised form
7 November 2015
Accepted 17 November 2015
Available online 14 January 2016

Keywords:
Fractal method
Geochemical data
Cu-Pb-Zn polymetallic deposits
Mineral exploration

ABSTRACT

Fractal and multi-fractal content area method finds application in a wide variety of geological, geochemical and geophysical fields. In this study, the fractal content-gradient method was used on 1:10,000 scale to delineate geochemical anomalies associated with copper mineralization. Analysis of geochemical data from the Yangla super large Cu-Pb-Zn polymetallic ore district using the fractal content-gradient method, combined with other geological data from this area, indicates that ore-prospecting in the ore district should focus on Cu as the main metal and Pb-Zn and Au as the auxiliary metals. The types of deposits include (in chronological order) re-formed sedimentary exhalative (SEDEX), skarns, porphyries, and hydrothermal vein-type deposits. Three ore-prospecting targets are divided on a S–N basis: (1) the Qulong exploration area, in which the targets are porphyry-type Cu deposits; (2) the Zongya exploration area, where the targets are porphyry-type Cu and hydrothermal vein-type Cu-Pb polymetallic deposits; and (3) the Zarelongma exploration area, characterized mainly skarn-type "Yangla-style" massive sulfide Cu-Pb deposits. Our study demonstrates that the fractal content-gradient method is convenient, simple, rapid, and direct for delineating geochemical anomalies and for outlining potential exploration targets.

1. Introduction

One of the most fundamental tasks of geochemical data processing is to determine the thresholds to separate anomalies from background values and then to identify the mineralized areas (Kürzl, 1988; Cheng and Li, 2002; Afzal et al., 2010; Bai et al., 2010; Hassanpour and Afzal, 2013; Zuo et al., 2013; Ahad Nazarpour et al., 2015). The main limitation of the classical approach is that it does not consider the spatial information, geometry (e.g., shape or form), extent and magnitude of the anomalous areas (Cheng et al., 1994) and fails to recognize anomalies in regions with high-value background or miss weak anomalies in region with known mineral deposits (Bai et al., 2010; Hassanpour and Afzal, 2013; Nazarpour et al., 2013). The fractal theory is one of the non-linear mathematical methods that was established by Mandelbrot (1983a,b) and widely used in many scientific fields including geosciences (Turcotte, 1986; Agterberg et al., 1993; Cheng et al., 1994; Carranza, 2008a,b; Deng et al., 2010; Wei and Yang, 2010; Sadeghi et al., 2012). Several fractal and multi-fractal models including concentration–area (C–A) (Cheng et al., 1994), spectrum–area (S–A) (Cheng et al., 2000a,b; Xu and Cheng, 2001; Cheng, 2004), concentration–distance (C–D) (Li et al., 2003), concentration–volume (C–V) (Afzal et al., 2010; Sadeghi et al., 2012), and number–size (N–S) (Mandelbrot, 1983a,b; Agterberg, 1995; Turcotte, 2002; Deng et al., 2010; Wang et al., 2010) have been developed for application in geosciences, especially in geochemical data processing.

In the past decades, numerous works have aimed at identifying geochemical anomalies using several methods (Harris et al., 1999, 2000; Mónica Arias et al., 2012), among which statistical methods are commonly used. These methods can be considered as non-

* Corresponding author. Tel.: +86 10 13910802638.
E-mail address: 3s@cugb.edu.cn (J. Chen).
Peer-review under responsibility of China University of Geosciences (Beijing).

http://dx.doi.org/10.1016/j.gsf.2015.11.010

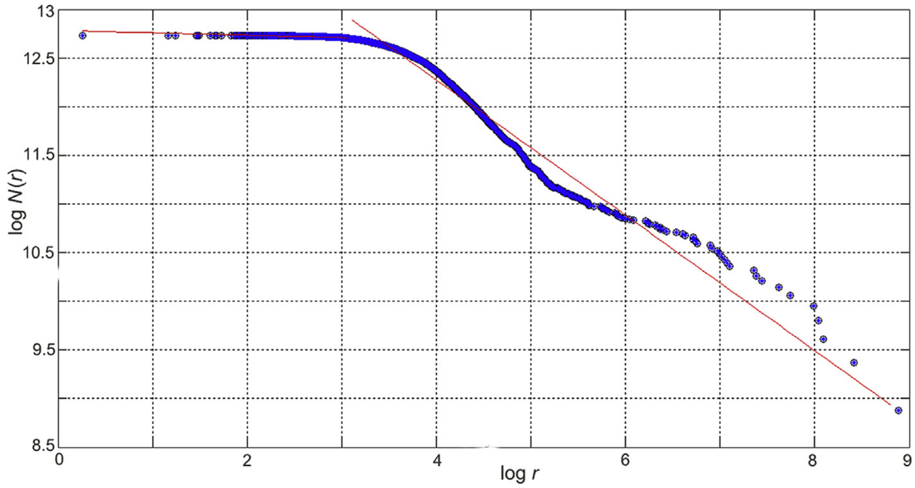

Figure 1. The fitted line intersection graph of the Cu anomaly threshold determined using the fractal method.

spatial statistical tools because they do not provide spatial information from geochemical data. In contrast, spatial statistical methods such as moving average techniques, kriging and spatial factor analysis (Grunsky and Agterberg, 1988) have been taken into account spatial correlation and variability among neighboring samples in addition to frequency distributions and correlation coefficients. These methods are effective for solving some problems but are of limited use in situations where weak anomalous values are hidden within the strong background variance (Cheng, 2007). Anomalous patterns caused by mineralizing processes are generally very complex in relation to their spatial and frequency properties. Accurate quantification of these spatial properties can be essential for identification of weak or complex anomalies and the tools available in Geographic Information. Systems (GIS) software is useful in this respect. Fractals and multifractal concepts have been applied to physical and chemical fields with geometrical support (e.g., Mandelbrot, 1977, 1983a,b; Mandelbrot et al., 1984). In the past two decades, several fractal/multi-fractal models supported by GIS have been developed and successfully applied to the study of the distribution of mineralization (e.g. Panahi and Cheng, 2004; Agterberg, 2007a,b; Carranza, 2008a; Ford and Blenkinsop, 2009; Gumiel et al., 2010; Arias et al., 2011) and as a powerful tool in the discrimination of geochemical anomalies (e.g., Cheng et al., 1994, 1996; Cheng, 1999; Gonçalves et al., 2001; Cheng, 2007; Carranza, 2008b, 2009, 2010a,b; Zuo and Cheng, 2008; Cheng and Agterberg, 2009; Deng et al., 2009, 2011; Zuo and Xia, 2009, 2011; Zuo et al., 2009a,b, 2010; Cheng et al., 2010; Wang et al., 2011; Zuo, 2011a,b,c, 2012). The aim of this paper is to contribute to the discrimination of geochemical anomalies, using the fractal content-gradient method, in the Yangla ore field and Cu-Pb-Zn mineralization.

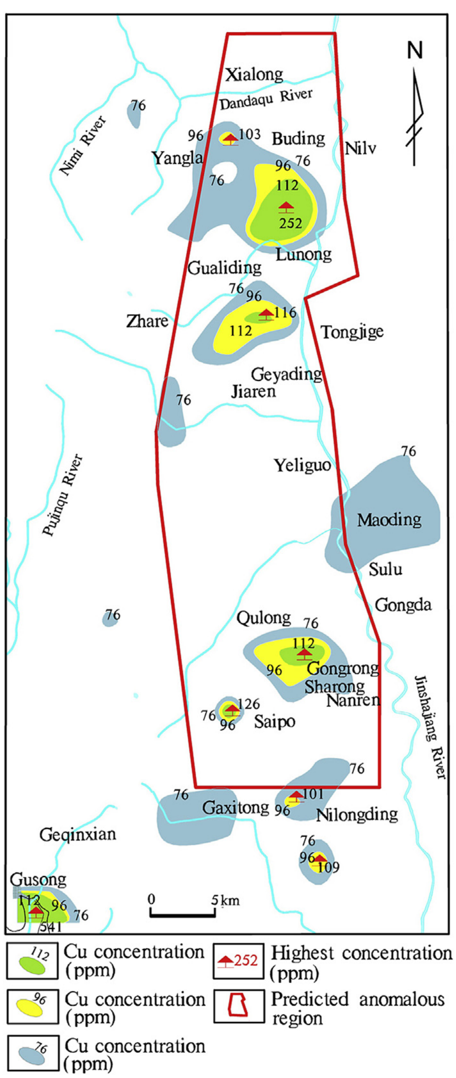

Figure 2. Cu element anomaly map.

2. Methodology

The fractal content-area method (KeGuo et al., 2007; Xu et al., 2013) establishes a content surface of the geochemical elements by interpolating their contents. The areas of the surfaces under different scales are then derived, and finally the thresholds of their geochemical anomalies are determined using the least squares method. The geochemically anomalous regions are delineated on the basis of the results. The method is used to delineate the geochemical anomaly concentration zones based on a conventional gradient concept. This method uses the derivable length of the bounded variation function and the fractal interpolation curve. The fractal interpolation is derived using a Hausdorff measure after delineating the anomalous regions. Specifically, the following steps are involved in this process:

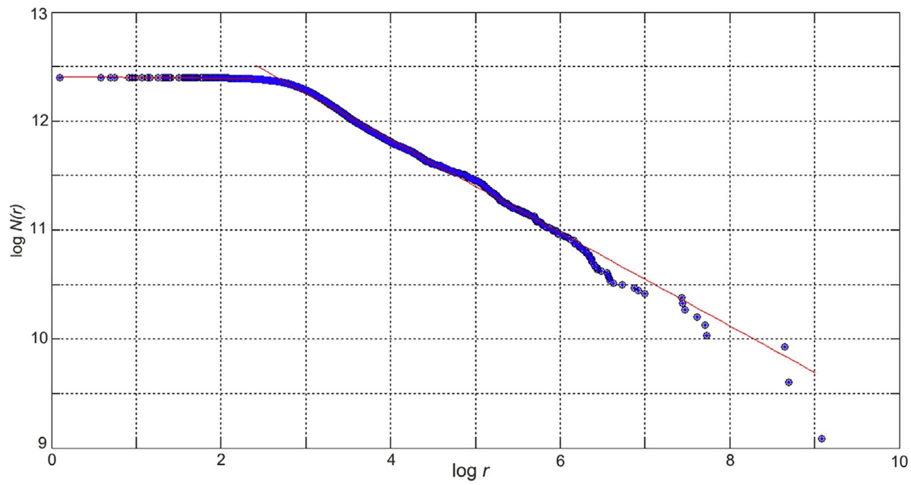

Figure 3. The fitted line intersection graph of the Pb anomaly threshold determined using the fractal.

Step 1: Interpolate the geochemical elements by ordinary kriging and generate a gridded content surface.

Step 2: Calculate the area of this content surface. If the content surface is rectangular when projected onto a plane, and if the contents of all four points on the surface are larger than the respective scale (under different content scales r), its area can be approximately expressed as

$$S_i(r) = \frac{1}{2}\left(\sqrt{Vx^2 + (h_{ai} - h_{bi})^2} \times \sqrt{Vy^2 + (h_{ai} - h_{di})^2} + \sqrt{Vx^2 + (h_{ci} - h_{di})^2} \times \sqrt{Vy^2 + (h_{ci} - h_{bi})^2}\right) \quad (1)$$

Otherwise as $S_i(r) = 0$.

Here, x and y are the geographical coordinates, and z is the element content at a point. Now, by summing the areas of all N small surfaces, the area of the entire content surface is

$$S(r) = \sum_{i=1}^{N} S_i(r) \quad (2)$$

Step 3: Calculate the content area $S(r)$ under different scales r. For different scales r, using

$$S(r) = K \cdot r^{2-D}, (r>0) \quad (3)$$

which yields a series of content areas $S(r)$. Here, K is a constant and D is a fractal dimension.

Step 4: Derive the anomaly thresholds of the geochemical elements and delineate the anomalous regions.

Logarithmizing both ends of Eq. (3), we get

$$\lg S(r) = -D \cdot \lg r + \lg K \quad (4)$$

This is a linear model relating to D. Because the anomaly threshold decides the low and high element content parts, these two parts are piecewise fitted by using least squares, and the geochemical anomaly threshold is the intersection between the two fitting lines. Thus, the geochemical anomalous region in the study area is delineated.

Step 5: Perform fractal interpolation to the content surface of elements within the delineated anomalous region to derive a fractal interpolation curve. Then, use planes respectively perpendicular to intersect the curve surface derived by fractional interpolation to produce fractal curves $S(X_i)$ and $S(Y_j)$.

Step 6: Determine the radius R. Take any point $M(t_0)$ from the fractal curve and two adjacent content extremes $M(t_1)$ and $M(t_2)$. $t_A = t_0 - t_1$, and, $t_B = t_2 - t_0$. To ensure that only two intersections exist between the radius R and the curve, we take $R = \min(|t_A|, |t_B|)$. Then, intersect the curve at t_1' andt_2' on a circle using t_0 as the center and R as the radius. Two special cases are

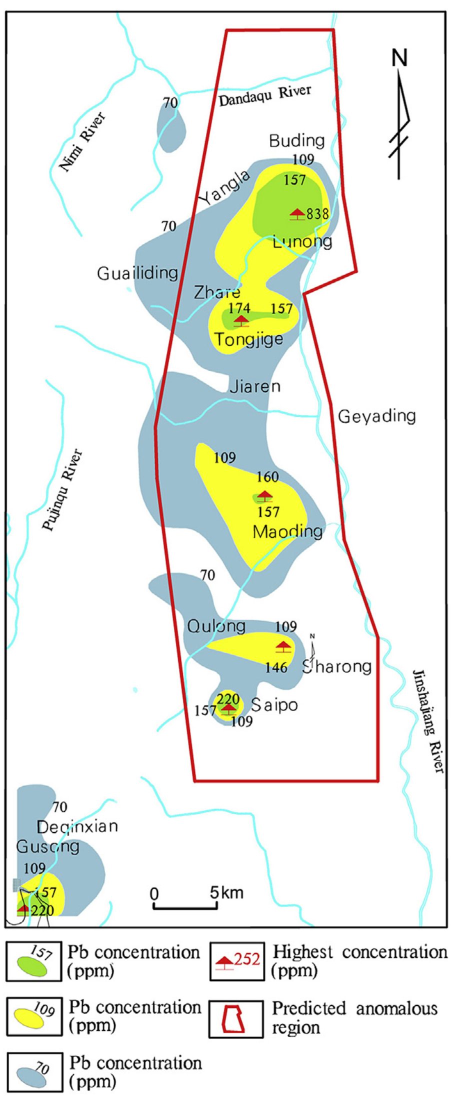

Figure 4. Pb element anomaly map method.

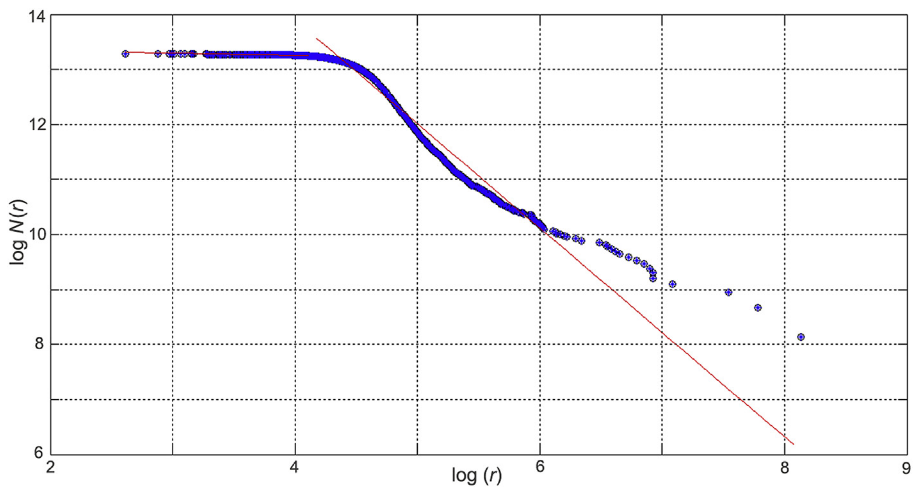

Figure 5. The fitted line intersection graph of the Zn anomaly threshold determined using the fractal method.

Table 1
Geochemical characteristics of stream sediments in the prediction area.

Element	Sample number	Weed out the number	Maximum	Minimum	Median	Background value	Anomaly threshold	Continental crust element content	Enrichment factor
Ag	451	117	6400.0	48.0	115.0	100.59	250.00	70.00	1.44
As	451	26	362.8	2.4	21.7	20.06	48.40	1.70	11.80
Au	448	46	27.7	0.3	2.0	1.80	5.00	2.50	0.72
Bi	443	49	39.8	0.1	0.4	0.32	0.90	0.08	4.05
Cu	451	19	932.8	11.5	48.2	45.57	83.30	25.00	1.82
Fe_2O_3	451	9	16.8	0.3	6.2	6.13	8.02	6.17	0.99
Hg	451	52	4685.0	7.0	35.0	31.13	80.00	40.00	0.78
K_2O	449	0	4.9	0.2	2.6	2.37	3.30	2.57	0.92
Mn	451	13	3634	109	882	857	1203	716	1.20
Mo	451	43	7.0	0.1	1.0	0.89	1.70	1.10	0.81
Pb	451	82	1500.0	4.8	30.4	27.52	72.50	14.80	1.86
Sb	451	28	29.7	0.2	1.9	1.66	3.70	0.30	5.54
Sn	451	47	20.6	1.0	3.5	3.23	4.80	2.30	1.40
Th	451	17	36.5	2.8	12.6	11.98	17.20	8.50	1.41
U	451	16	16.9	0.1	2.5	2.40	4.10	2.60	0.92
W	451	64	109.5	0.4	1.9	1.70	3.80	1.00	1.70
Zn	451	66	828.6	32.5	93.6	88.21	131.60	65.00	1.36

Note: Au, Ag, and Hg are expressed in ppb. Fe_2O_3 and K_2O are expressed in wt.%. The remaining elements are expressed in ppm. The contents of continental crust elements are quoted from K. H. Wedepohl. The background values are the statistical means after deducting twice the logarithmic standard deviation. The anomaly threshold is the value corresponding to 85% cumulative frequency.

considered: when $R = |t_A|$, $t_1^{'} = t_1$ and $t_2^{'} = t_0 + t_A$; when $R = |t_B|$, $t_1^{'} = t_0 - t_B$, $t_2^{'} = t_2$.

Step 7: Derive the content gradient of the geochemical content. Take any point $S(t_0) \in S(X_i)$ from the fractal curve. Then, the content gradient of the element under the Hausdorff measure is

$$G_H^{(s)} = \frac{|S(t_1^{'}) - S(t_2^{'})|^s}{|2R|^s} \tag{5}$$

Table 2
Element associations and anomaly interpretation based on multivariate statistical analysis of stream sediment.

Main factor	Main element associations	Anomaly interpretation and geological significance
1	Cu, Bi, W, Zn, Hg, Ag	Indicator of the metallogenic processes of Cu deposits
2	U, Th, K_2O	Indicator of the extent of intermediate-acidic rock bodies in the prediction area
3	Pb, As	Indicator of acidic rock bodies and their metallogenesis
4	Au	Indicator of Au mineralization processes

where $S(t)$ is the functional expression of curve $S(X_i)$ and S is the Hausdorff fractal dimension of the curve.

Step 8: Determine the anomaly concentration zone. Calculate the gradient of each element within the anomalous region in the study area, and determine the weighted average of the maximum gradient of each element to obtain the intra-zone boundary value of this anomalous region. Using the weighted average of the gradients of the elements in the anomalous region that are not larger than this inter-zone boundary value, we can obtain the intra-zone boundary value. Thus, it is possible to determine the anomaly concentration zone. From the intersection between the planes, we get the fractal curves $S(X_i)$ and $S(Y_j)$.

3. Case study

3.1. Geological setting of the Yangla ore field

The ore district lies in the Jinshajiang plate junction and the northern segment of Weixi–Luchun late Paleozoic to early Mesozoic volcanic arcs. In this area, the Weixi–Luchun volcanic arcs

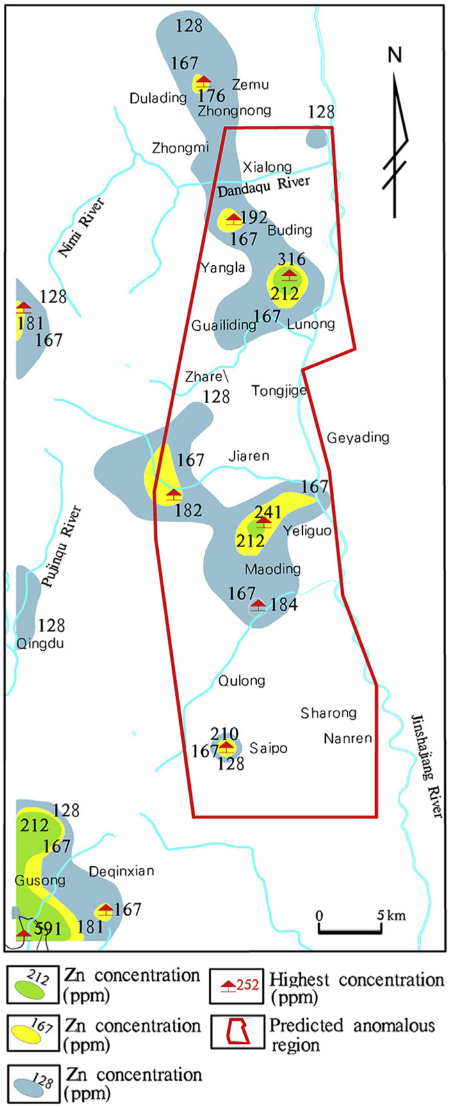

Figure 6. Zn element anomaly map.

(including a part of the intra-oceanic arc) are connected in the form of a mosaic superposition among Permian and Triassic volcanic arcs and back-arc basins of various nature. Westward subduction of the Jinshajiang Oceanic Plate in the early Permian resulted in the formation of a series of thrust faults that formed during a dynamic transition from compression to extension (Yang et al., 2014). The fault system provided favorable pathways for the magmas and ore-forming fluids generating the Yangla deposit (Yang et al., 2014).

Among the Jinshajiang faults, a group of NE λ-shaped secondary faults occur that generally strike 45–60° and range in size from 5 to 10 km to a few 10 m; their surfaces dip NW at 60–80°. These faults represent important migration passages for ore-bearing hydrothermal fluids. The fractured rocks along the faults display signs of argillation, carbonatization, propylitization, and different intensities of pyritization and chalcopyritization.

The prospect area is the Jinshajiang fold zone. Its constraint on metallogenesis is typically reflected by an interformational detachment at the contacts of formations of various lithologies and the development of interformational fissures and fracture zones. These conditions provide migration and storage spaces for ore-forming solutions such as the transition of Cu deposits between the Yubo anticline and syncline.

Magmatic processes are primarily of Variscan and Indosinian–Yanshanian ages. The former is the source of volcanic rocks such as hornblende andesite and basalt, whereas the latter is responsible for intermediate-acidic intrusive rocks that are closely related to metallogenesis. The Linong rock intrusion occurs between Linong and Jiangbian members and occur in the form of stocks intruding the core of the Linong dome. The central phase of the rock body is medium- to coarse-grained granodiorite, and the marginal phase is medium- to fine-grained adamellite. The wall-rock is composed of rocks from the Linong and Jiangbian formations.

Sulfur isotope compositions of sulfide minerals (pyrite, chalcopyrite, pyrrhotite, and molybdenite) from the main and late ore stage show a narrow range with $\delta^{34}S$ values from −1.9 to 2.6‰, consistent with a magmatic origin (Zhu et al., 2015). Lead isotope compositions of sulfides ($^{206}Pb/^{204}Pb$ = 18.273–18.369, $^{207}Pb/^{204}Pb$ = 15.627–15.677, and $^{208}Pb/^{204}Pb$ = 38.445–39.611) are similar to those of the granitic intrusions and sedimentary wall rocks, but distinct from those of basalts (Zhu et al., 2015). Garnet, diopside, quartz, and calcite are associated in the skarn ore. Fluid inclusion study (Zhu et al., 2015) suggests three stages for ore-forming fluids as follows: (1) early fluids trapped at temperatures of 560–600 °C, with average salinity of 49.4 ± 1.7 wt.% NaCl eq.; (2) main ore stage represented by vapor- and liquid-rich fluid inclusions; the liquid-rich inclusions homogenize between 312 and 389 °C, with salinities of 2.4–5.6 wt.% NaCl eq.; (3) late ore stage fluid inclusions trapped at 220–290 °C and having salinities between 2.1 and 8.0 wt.% NaCl eq.

Based on these characteristics, we classify the genesis of the deposits in this area as pneumatolytic–hydrothermal deposits associated with the Indosinian–Yanshanian magmatic porphyries. Chalcopyrite-bearing felsic veinlets and ouralite and chlorite veinlets from the various stages indicate multiple replacements. Multiple medium- and low-temperature hydrothermal events superposing the metallogenic process are believed to have occurred after the skarn-type Cu (the main orebody) was formed during the earlier pneumatolytic–hydrothermal period.

3.2. Identifying geochemical anomalies

A total of 5169 geochemical samples were collected. Six elements, i.e., Cu, Pb, Zn, Ag, Au and Sb, were analyzed (Figs. 1–5). In this section, descriptions of the geochemical characteristics of these elements are given.

(1) Geochemical parameter characteristics

Table 1 shows the geochemical characteristics of the elements in the Jiaren ore-prediction area. As, Sb, and Bi are highly concentrated in this area, with concentration factors larger than 4, and Pb, Cu, W, Ag, Th, Sn, Zn, and Mn are moderately concentrated, with concentration factors larger than 1.2. Fe_2O_3, K_2O, and U are less concentrated, and relatively diluted elements include Mo, Hg, and Au. Multivariate statistical analysis was performed on data obtained in the ore-prediction area. The factorial analysis results are given in Table 2.

(2) The fractal content-area method to determine the thresholds of their geochemical anomalies

Cu, Pb, and Zn are the main elements in the study area, and we used the mean + two times the standard deviation for anomaly threshold, two times the anomaly threshold for middle belt, four times the anomaly threshold of traditional delineation of

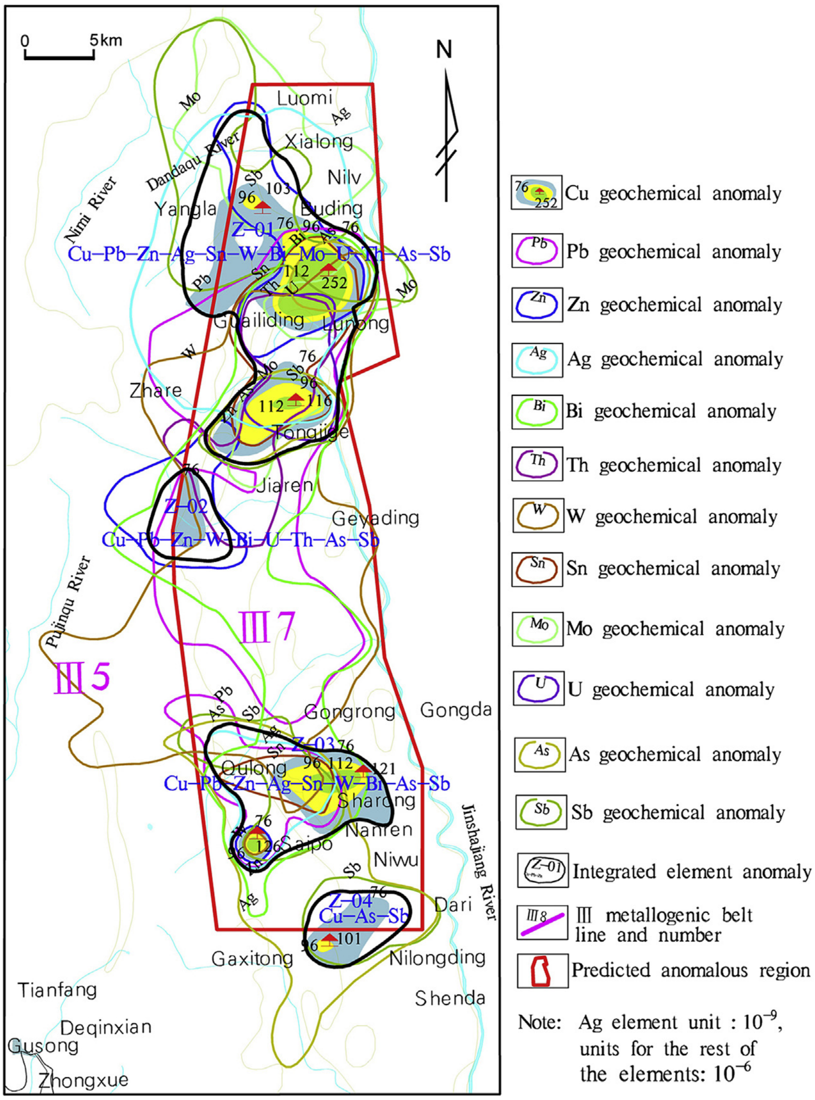

Figure 7. Cu-Pb-Zn-Ag-Bi-Th-W geochemical composite anomaly map in the prediction area.

concentration points coupled with gradient method and fractal content to calculate the element zoning sequence (Figs. 1, 3 and 5.)

(3) Geochemical anomaly characteristics

The geochemical anomalies of Cu are typically detected at the contact between the granodiorite and adamellite formations and fit well into the Cu deposits. Thus, the acidic rock-related skarn-type Cu deposits must be given more focus (Fig. 2). The geochemical anomalies of Au elements are typically detected in Zhongnong and Qulong and are mainly related to formation type, felsic nature, and contact location (Fig. 7). The geochemical anomalies of Pb and Zn are arranged similar along linear bands. They typically overlie acidic rocks and contacts and are oriented in the same directions as those of the acidic rocks, representing close genetic link (Figs. 4 and 6). The geochemical anomalies of U and Sn appear to overlie gabbro and acidic rock bodies at the contacts. The geochemical anomalies of U are oriented in the same direction as that of the gabbro. The geochemical anomalies of Ag are typically detected in the ore district. The geochemical anomalies of As, Sb, and Hg are spread along faults and are related to faulting activities (Fig. 8). Mo is found in acidic rock bodies, contacts of the acidic rock bodies and formations, and within formations. Its geochemical anomalies are similar to those of Au.

According to the ore-prospecting prediction map of the ore district, three targets areas are delineated: (a) the Qulong exploration area, in which the targets are porphyry-type Cu deposits; (b) the Zongya exploration area, in which the targets are porphyry-type Cu and hydrothermal vein-type Cu–Pb polymetallic deposits; and (c) the Zarelongma exploration area, in which the targets are mainly skarn-type “Yangla-style” massive sulfide Cu–Pb deposits with focus also on skarn and hydrothermal-type deposits (Fig. 9).

Pb-Zn deposits in Geyading are brought out in the anomalies. In the Rongdegong and Qulong anomalies, new Cu and Au polymetallic deposits have been detected.

4. Discussion and conclusions

The 1:10,000 soil geochemical data on elements Cu, Pb, Zn, Ag, Au and Sb in and around the Cu deposits were analyzed. The geochemically anomalous regions of each element were delineated

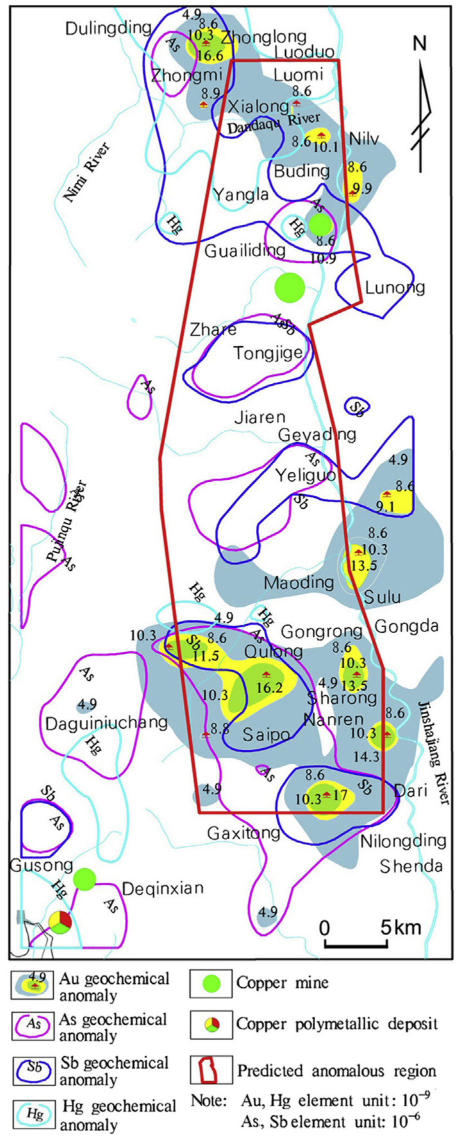

Figure 8. Au-As-Sb-Hg Geochemical composite anomaly map in the prediction area.

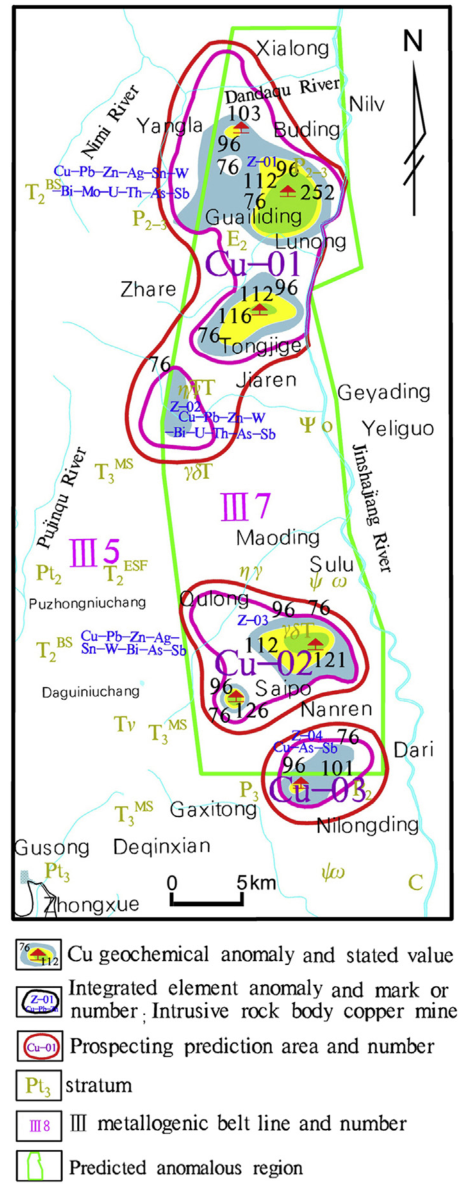

Figure 9. Ore-prospecting prediction map of ore district.

using the fractal content-area method. Within these regions, the anomaly concentration center of each element was delineated using the fractal content-gradient method to determine the anomaly zoning characteristics and to suggest further ore-prospecting efforts in this area.

Well-fit elements at the Cu occurrences include Cu, Ag, Bi, Pb, Zn, Sn, and W. Their anomalies are characterized by large size, high intensity, obvious concentration centers, and three-level concentration zones. Less well-fit elements include Mo, As, Sb, Au, Th, and U, which display two-level concentration zones. The W, Pb, Bi, Sn, Th, and U anomalies are oriented in the same direction as that of the granodiorite.

Ore-prospecting in the ore district should focus on Cu as the main metal and Pb-Zn and Au as the auxiliary metals. In chronological order, the deposit types include re-formed sedimentary exhalative deposits (SEDEX,) skarns, porphyries, and hydrothermal vein type deposits. Three ore-prospecting targets are divided on a south-to-north basis: (a) the Qulong exploration area, in which the targets are porphyry-type Cu deposits; (b) the Zongya exploration area, in which the targets are porphyry-type Cu and hydrothermal vein-type Cu-Pb polymetallic deposits; and (c) the Zarelongma exploration area, in which the targets are mainly skarn-type "Yangla-style" massive sulfide Cu-Pb deposits, with focus also on skarns and hydrothermal-type deposits.

The method also can be applied to other polymetallic mineralization elsewhere in the world.

Acknowledgments

The authors sincerely thank two reviewers for their critical reviews and constructive comments which have greatly improved the manuscript. This study was supported by the fund "Metallogenic Geodynamic Background, Process and Quantitative Evaluation of Super Large Fe-Cu Polymetallic Deposits, Qinghai Qimantag Area" (Grant No. 1212011220929) from Beijing Key Laboratory of Land Resources Information Research and Development, China University of Geosciences, Beijing.

References

Afzal, P., Khakzad, A., Moarefvand, P., Omran, N.R., Esfandiari, B., Alghalandis, Y.F., 2010. Geochemical anomaly separation by multifractal modeling in Kahang (Gor Gor) porphyry system, Central Iran. Journal of Geochemical Exploration 104, 34–46.
Agterberg, F.P., 1995. Multifractal modeling of the sizes and grades of giant and super-giant deposits. International Ore Geology Reviews 37, 1–8.
Agterberg, F.P., 2007a. Mixtures of multiplicative cascade models in geochemistry. Nonlinear Processes in Geophysics 14, 201–209.
Agterberg, F.P., 2007b. New applications of the model of de Wijs in regional geochemistry. Mathematical Geology 39, 1–25.
Agterberg, F., Cheng, Q., Wright, D., 1993. Fractal modeling of mineral deposits. In: 24th APCOM Symposium Proceeding, Montreal, Canada, pp. 43–53.
Arias, M., Gumiel, P., Sanderson, D.J., Martin-Izard, A., 2011. A multifractal simulation model for the distribution of VMS deposits in the Spanish segment of the Iberian Pyrite Belt. Computers and Geosciences 37, 1917–1927.
Arias, M., Gumiel, P., Martín-Izard, Agustín, 2012. Multifractal analysis of geochemical anomalies: A tool for assessing prospectivity at the SE border of the Ossa Morena Zone, Variscan Massif (Spain). Journal of Geochemical Exploration 122, 101–112.
Ahad, Nazarpour., Nematolah, Rashidnejad Omran, Ghodratolal, Rostami Paydar, Behnam, Sadeghi, Fatemeh, Matroud, Ali, Mehrabi Nejad, 2015. Application of classical statistics, logratio transformation andmultifractal approaches to delineate geochemical anomalies in the Zarshuran gold district, NW Iran. Chemie der Erde 75, 117–132.
Bai, J., Porwal, A., Hart, C., Ford, A., Yu, L., 2010. Mapping geochemical singularity using multifractal analysis: application to anomaly definition on stream sediments data from Funin Sheet, Yunnan, China. Geochemistry: Exploration, Environment, Analysis 104, 1–11.
Carranza, E.J.M., 2008a. Controls on mineral deposit occurrence inferred from analysis of their spatial pattern and spatial association with geological features. Ore Geology Reviews 35, 383–400.
Carranza, E.J.M., 2008b. Geochemical Anomaly and Mineral Prospectivity Mapping in GIS. In: Handbook of Exploration and Environmental Geochemistry, vol. 11. Elsevier, Amsterdam.
Carranza, E.J.M., 2009. Mapping of anomalies in continuous and discrete fields of stream sediment geochemical landscapes. Geochemistry: Exploration, Environment, Analysis 10, 171–187.
Carranza, E.J.M., 2010a. Mapping of anomalies in continuous and discrete fields of stream sediment geochemical landscapes. Geochemistry: Exploration, Environment, Analysis 10, 171–187.
Carranza, E.J.M., 2010b. Catchment basin modeling of stream sediment anomalies revisited: incorporation of EDA and fractal analysis. Geochemistry: Exploration, Environment, Analysis 10, 365–381.
Cheng, Q., 1999. Multifractality and spatial statistics. Computers and Geosciences 25, 949–961.
Cheng, Q., 2004. A new model for quantifying anisotropic scale invariance and fordecomposition of mixing patterns. Mathematical Geology 36, 345–360.
Cheng, Q., 2007. Mapping singularities with stream sediment geochemical data for prediction of undiscovered mineral deposits in Gejiu, Yunnan Province, China. Ore Geology Reviews 32, 314–324.
Cheng, Q., Li, Q., 2002. A fractal concentration-area method for assigning a color palette for image representation. Computers Geoscience 28, 567–575.
Cheng, Q., Agterberg, F.P., 2009. Singularity analysis of ore-mineral and toxic trace elements in stream sediments. Computers and Geosciences 35, 34–244.
Cheng, Q., Agterberg, F., Ballantyne, S., 1994. The separation of geochemical anomalies from background by fractal methods. Journal of Geochemistry: Exploration, Environment, Analysis 51, 109–130.
Cheng, Q., Agterberg, F.P., Bonham-Carter, G.F., 1996. A spatial analysis method for geochemical anomaly separation. Journal of Geochemical Exploration 56, 183–195.
Cheng, Q., Xu, Y., Grunsky, E., 2000a. Multifractal power spectrum-area method for geochemical anomaly separation. Natural Resources Research 9, 43–51.
Cheng, Q., Xu, Y., Grunsky, E., 2000b. Integrated spatial and spectrum method for geochemical anomaly separation. Natural Resources Research 9 (1), 43–52.
Cheng, Q., Xia, Q., Li, W., Zhang, S., Chen, Z., Zuo, R., Wang, W., 2010. Density/area power-law models for separating multi-scale anomalies of ore and toxic elements in stream sediments in Gejiu mineral district, Yunnan Province, China. Biogeosciences 7, 3019–3025.
Deng, J., Wang, Q., Wan, L., Yang, L., Gong, Q., Zhao, J., Liu, H., 2009. Self-similar fractal analysis of gold mineralization of Dayingezhuang disseminated-veinlet deposit in Jiaodong gold province, China. Journal of Geochemical Exploration 102, 95–102.
Deng, J., Wang, Q., Yang, L., Wang, Y., Gong, Q., Liu, H., 2010. Delineation and explanation of geochemical anomalies using fractal models in the Heqing area, Yunnan Province, China. Journal of Geochemical Exploration 105, 95–105.
Deng, J., Wang, Q.F., Wan, L., Liu, H., Yang, L.Q., Zhang, J., 2011. A multifractal analysis of mineralization characteristics of the Dayingezhuang disseminated-veinlet gold deposit in the Jiaodong gold province of China. Ore Geology Reviews 40, 54–64.
Ford, A., Blenkinsop, T.G., 2009. An expanded de Wijs model for multifractal analysis of mineral production data. Mineralium Deposita 44, 233–240.
Gonçalves, M.A., Mateus, A., Oliveira, V., 2001. Geochemical anomaly separation by multifractal modeling. Journal of Geochemical Exploration 72, 91–114.
Grunsky, E.C., Agterberg, F.P., 1988. Spatial and multivariate analysis of geochemical data from metavolcanic rocks in the Ben Nevis Area, Ontario. Mathematical Geology 7, 415–446.
Gumiel, P., Sanderson, D.J., Arias, M., Roberts, S., Martín-Izard, A., 2010. Analysis of the fractal clustering of ore deposits in the Spanish Iberian Pyrite Belt. Ore Geology Reviews 38, 307–318.
Harris, J.R., Wilkinson, L., Grunsky, G., Heather, K., Ayer, J., 1999. Techniques for analysis and visualization of lithogeochemical data with applications to the Swayze greenstone belt, Ontario. Journal of Geochemical Exploration 67, 301–334.
Harris, J.R., Grunsky, E.C., Wilkinson, L., 2000. Effective use and interpretation of lithogeochemical data in regional exploration programs. Ore Geology Reviews 16, 107–143.
Hassanpour, S., Afzal, P., 2013. Application of concentration-number (C-N) multifractal modeling for geochemical anomaly separation in Haftcheshmeh porphyry system, NW Iran. Arab Journal Geoscience 6, 957–970.
Li, C., Ma, T., Shi, J., 2003. Application of a fractal method relating concentrations and distances for separation of geochemical anomalies from background. Journal of Geochemical Exploration 77, 167–175.
KeGuo, Chen, L., Tang, J.X., 2007. Research on nonlinear geochemical anomaly recognition in complex geological and Geomorphological areas. Journal of Chengdu University of Technology (Natural Sciences Edition) 34 (6), 599–604 (in Chinese).
Kürzl, H., 1988. Exploratory data analysis: recent advances for the interpretation of geochemical data. Journal of Geochemical Exploration 30, 309–322.
Mandelbrot, B.B., 1977. Fractals: Form, Chance, and Dimension. Freeman, San Francisco, 365 pp.
Mandelbrot, B.B., 1983a. The Fractal Geometry of Nature. Macmillan.
Mandelbrot, B.B., 1983b. The Fractal Geometry of Nature, Updated and Augmented Edition. Freeman, New York, 468 pp.
Mandelbrot, B.B., Passoja, D.E., Paullay, A.J., 1984. Fractal character of fracture surfaces of metals. Nature 308 (5961), 721–722.
Nazarpour, A., Omran, N.R., Paydar, G.R., 2013. Application of multifractal modelsto identify geochemical anomalies in Zarshuran Au deposit, NW Iran. Arabian Journal of Geosciences 1–13.
Panahi, A., Cheng, Q., 2004. Multifractality as a measure of spatial distribution of geochemical patterns. Mathematical Geology 36, 827–846.
Sadeghi, B., Moarefvand, P., Afzal, P., Yasrebi, A.B., Saein, L.D., 2012. Application of fractal models to outline mineralized zones in the Zaghia iron ore deposit, Central Iran. Journal of Geochemical Exploration 122, 9–19.
Turcotte, D.L., 1986. A fractal approach to the relationship between ore grade and tonnage. Economic Geology 81, 1528–1532.
Turcotte, D.L., 2002. Fractals in petrology. Lithos 65, 261–271.
Wang, Q., Deng, J., Liu, H., Yang, L., Wan, L., Zhang, R., 2010. Fractal models for ore reserve estimation. Ore Geology Reviews 37, 2–14.
Wang, Q., Deng, J., Wan, L., Zhang, Z., 2011. Fractal analysis of the ore-forming process in a skarn deposit: a case study in the Shizishan area, China. In: Sial, A.N., Bettencourt, J.S., De Campos, C.P., Ferreira, V.P. (Eds.), Granite-related Ore Deposits. Geological Society, London, Special Publications 350, pp. 89-104.
Wei, B., Yang, L., 2010. A review of heavy metal contaminations in urban soils, urban road dusts and agricultural soils from China. Microchemical Journal 94, 99–107.
Xu, Y., Cheng, Q., 2001. A fractal filtering technique for processing regional geochem-ical maps for mineral exploration. Geochemistry: Exploration, Environment, Analysis 1, 147–156.
Xu, B., Wang, Q.F., Liu, B., Chang, X., Zhang, X.P., 2013. Application of fractal content-gradient method for delineating geochemical anomalies. Journal of Anhui Normal University (Natural Science) 36 (6), 573–577 (in Chinese).
Yang, Xi-An, Liu, Jia-Jun, Yang, Long-Bo, Han, Si-Yu, Sun, Xiao-Ming, Wang, Huan, 2014. Fluid inclusion and isotope geochemistry of the Yangla copper deposit, Yunnan, China. Mineralogy and Petrology 108, 303–315.
Zhu, J.J., Hu, R.Z., Richards, J.P., Bi, X.W., Zhong, H., 2015. Genesis and magmatic-hydrothermal evolution of the Yangla Skarn Cu Deposit, Southwest China. Economic Geology 110, 631–652.
Zuo, R., 2011a. Decomposing of mixed pattern of arsenic using fractal model in Gangdese belt, Tibet, China. Applied Geochemistry 26, S271–S273.
Zuo, R., 2011b. Identifying geochemical anomalies associated with Cu and Pb/Zn skarn mineralization using principal component analysis and spectrum-area fractal modeling in the Gangdese Belt, Tibet (China). Journal of Geochemical Exploration 111, 13–22.
Zuo, R., 2011c. Regional exploration targeting model for Gangdese porphyry copper deposits. Resource Geology 61, 296–303.
Zuo, R., 2012. Exploring the effects of cell size in geochemical mapping. Journal of Geochemical Exploration 112, 357–367.
Zuo, R., Cheng, Q., 2008. Mapping Singularities: a Technique to Identify Potential.

Zuo, R., Xia, Q., 2009. Application fractal and multifractal methods to mapping prospectivity for metamorphosed sedimentary iron deposits using stream sediment geochemical data in eastern Hebei province, China. Geochimica et Cosmochimica Acta 73, A1540–A1540.

Zuo, R., Cheng, Q., Agterberg, F.P., Xia, Q., 2009a. Application of singularity mapping technique to identification local anomalies using stream sediment geochemical data, a case study from Gangdese, Tibet, Western China. Journal of Geochemical Exploration 101, 225–235.

Zuo, R., Cheng, Q., Xia, Q., 2009b. Application of fractal models to characterization of vertical distribution of geochemical element concentration. Journal of Geochemical Exploration 102, 37–43.

Zuo, R., Xia, Q., Wang, H., 2013. Compositional data analysis in the study of integrated geochemical anomalies associated with mineralization. Applied Geochemistry 28, 202–211.